

Innovation: Searching for Galileo

Reception and Analysis of Signals from GIOVE-A

Jun 1, 2006

By: [Mark L. Psiaki](#), [Todd E. Humphreys](#), [Shan Mohiuddin](#), [Steven P. Powell](#), [Alessandro P. Cerruti](#), [Paul M. Kintner, Jr.](#)

GPS World

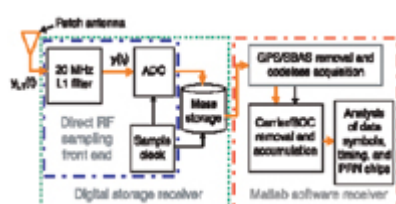
Galileo, Europe's answer to the U.S. Global Positioning System, achieved a milestone on December 28, 2006, with the launch of its first test satellite, GIOVE-A, which began transmitting navigation signals in early January 2006. Since the launch, receiver developers around the world have been anxious to test their Galileo-capable receivers on the GIOVE-A signals. But because the GIOVE-A signal structure documentation had not yet been publicly released, only approved groups involved in validation tests had authorized access to the pseudorandom noise (PRN) codes required to track the GIOVE-A navigation signals.

Eager to study the Galileo signals and to develop Galileo-capable receivers, Cornell University's GNSS research group set out to determine whether the GIOVE-A L1 binary offset carrier - BOC(1,1) - signal could be acquired and the PRN codes uncovered using codeless acquisition and statistical signal processing techniques. The short answer: Yes!

We recorded data using a digital storage receiver connected to an inexpensive roof-mounted patch antenna on Cornell University's campus in Ithaca, New York. We then processed the data offline in several stages. First, the "nuisance" GPS and satellite-based augmentation system (SBAS) - WAAS and EGNOS - C/A-code signals were tracked and removed. Then the GIOVE-A L1 BOC(1,1) signal's carrier phase, Doppler shift, and BOC phase were determined using codeless acquisition techniques. Next, the carrier and BOC signals were removed by mixing, and 1.023 MHz in-phase accumulations were computed. Finally, the code timing, data symbols, and secondary code chips were analyzed and the results were used to accurately determine the primary PRN codes by averaging over many code periods.

The resulting PRN codes can be obtained online at <http://gps.ece.cornell.edu/galileo/>.

Signal Data



We captured the GIOVE-A BOC(1,1) signal using the digital storage receiver illustrated in **FIGURE 1**. It employed a 20 MHz L1 filter and direct radio frequency (RF) sampling at 41.19 MHz to alias the L1 GPS/Galileo signals to the nominal intermediate frequency $f_{IF} = 10.36$ MHz.

Figure 1 Schematic block diagram of the data recording hardware and the post-processing software receiver. The two data sets used in our study, captured on March 2 at 14:45:10 UTC and on March 8 at 09:29:00 UTC, were taken when GIOVE-A was visible both from Ithaca and from Europe during European business hours - a measure taken to increase the likelihood that the satellite was broadcasting. The flyovers were predicted using NORAD two-line ephemeris elements.

Two Lobes. The power spectrum of the raw data from the digital storage receiver is shown as the red dashed line in **FIGURE 2**. The combined power of several GPS/SBAS C/A-code signals is evident in the large hump centered at f_{IF} . These GPS/SBAS signals interfere with codeless acquisition and analysis of the Galileo L1 BOC(1,1) signal. In addition, they obscure the GIOVE-A signal in the power spectrum, thereby precluding a quick test for its presence.

We used a software GPS receiver to acquire, track, and remove the nuisance GPS/SBAS signals. This procedure removes the large central hump in the power spectrum, revealing distinct lobes to each side of the intermediate frequency - the expected signature of the Galileo L1 signal's BOC(1,1) modulation.

Signal Structure

Our analysis required a detailed understanding of the Galileo L1 signal structure. We pieced together a coherent signal description from early, publicly available drafts of the Galileo Interface Control Document (ICD). Our later findings demonstrated that these documents were a generally accurate description of the GIOVE-A signal, with a few important exceptions. In this section, we present the GIOVE-A L1 BOC(1,1) signal structure as we detected it.

The BOC(1,1) signal is composed of two multiplexed channels: the L1-B data channel and the L1-C pilot channel. The sampled Galileo L1 BOC(1,1) signal that exits at the RF front-end takes the form

$$y_i = A[b_{L1-B}(\tau_i)d_{L1-B}(\tau_i) - c_{L1-C}(\tau_i)s_{L1-C}(\tau_i)] s_{SC}(\tau_i) \cos(2\pi f_{IF}\tau_i + \phi_0) + v_i \quad (1)$$

at receiver sample time t_i . The quantities in Equation (1) are the carrier amplitude A , the PRN code of the data channel $b_{L1-B}(\tau_i)$, the data symbol $d_{L1-B}(\tau_i)$, the primary PRN code of the pilot channel $c_{L1-C}(\tau_i)$, the secondary code of the pilot channel $s_{L1-C}(\tau_i)$, the sine-phased BOC signal $s_{SC}(\tau_i) = \text{sign}[\sin(2\pi f_{BOC}\tau_i)]$ where f_{BOC} is the BOC(1,1)

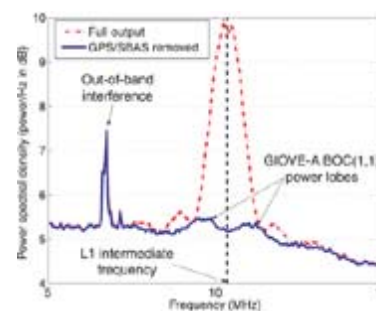


Figure 2 L1-band power spectral densities, raw data, and data after removal of GPS and SBAS L1 C/A-code signals

modulation frequency equal to 1.023 MHz, the initial carrier phase ϕ_0 , the measurement noise and the signal transmission time τ_i . This latter time can be expressed as a quadratic polynomial with a constant term that depends on pseudorange and linear and quadratic terms that depend on carrier Doppler shift and Doppler shift rate.

The PRN codes and the data time history in Equation (1) take the form

$$b_{L1-B}(\tau_i) = \sum_{n=0}^{\infty} b_{\text{mod}(n,4092)} \Pi_{T_c}(\tau_i - nT_c) \tag{2a}$$

$$d_{L1-B}(\tau_i) = \sum_{n=0}^{\infty} d_n \Pi_{T_d}(\tau_i - nT_d) \tag{2b}$$

$$c_{L1-C}(\tau_i) = \sum_{n=0}^{\infty} c_{\text{mod}(n,8184)} \Pi_{T_c}(\tau_i - nT_c) \tag{2c}$$

$$s_{L1-C}(\tau_i) = \sum_{n=0}^{\infty} s_{\text{mod}(n,25)} \Pi_{T_s}(\tau_i - nT_s) \tag{2d}$$

where b_0, \dots, b_{4091} is the PRN of the L1-B data channel, d_0, d_1, \dots is the navigation data symbol sequence, c_0, \dots, c_{8183} is the PRN code for the L1-C pilot channel and s_0, \dots, s_{24} is the secondary code for the pilot channel. The sequence elements take on ± 1 values. The function $\Pi_T(t)$ is a usual rectangular support function equal to one over the interval $0 < t < T$ and zero elsewhere.

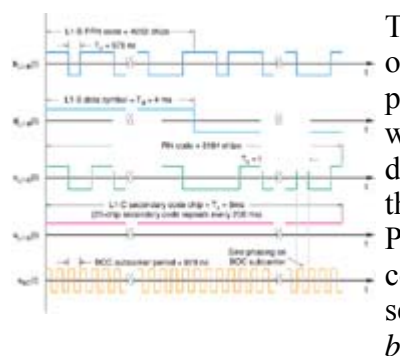


Figure 3 Timing diagram of components of GIOVE-A L1 BOC(1,1) signal

s_0, \dots, s_{24} . The nominal chipping/symbol rates for these sequences are $1/T_c = 1.023$ MHz for the L1-B PRN code and the L1-C primary PRN code, $1/T_d = 250$ Hz for the L1-B data symbols, $1/T_s = 125$ Hz for the L1-C secondary PRN code. The L1-B PRN code has a nominal period of 4 milliseconds. The combined L1-C PRN code has a nominal period of 200 milliseconds. **FIGURE 3** is a graphical representation of the data symbols and PRN codes.

Codeless Signal Acquisition

Acquiring the GIOVE-A L1 BOC(1,1) signal is a straightforward process if the L1-B and L1-C PRN codes are known. When the PRN codes are unknown, codeless signal acquisition techniques are invoked to estimate the Doppler shift, carrier phase, and BOC phase of the signal.

Acquisition Statistic. We acquired the GIOVE-A signal by maximizing an acquisition statistic. The acquisition statistic was computed based on two types of in-phase and quadrature accumulations. The first type of accumulations were computed after mixing to baseband using the BOC signal $s_{SC}(\tau_i)$ and the

phase and quadrature carrier replicas $\cos(2\pi f_{IF} \tau_i)$ and $\sin(2\pi f_{IF} \tau_i)$. The BOC phase, the Doppler shift, and the Doppler shift rate were used implicitly in this calculation because they affected the computation of the broadcast time τ_i as a function of the sample time t_i . The accumulations were computed at the nominal 1.023 MHz chipping rate of the L1-B and L1-C PRN codes, and they were aligned with the chip intervals as defined by the

$$\Pi_{T_c}(\tau_i - nT_c)$$

functions in Equations (2a) and (2b).

The accumulations of the second type exploited the observed 200-millisecond periodicity of the total L1-C pilot PRN code by summing first-type accumulations with time indices j , $j+204600$, $j+409200$, ... into a single second-type accumulation. There were 204,600 of these new accumulations, and they increased the signal detection power of the acquisition along with its sensitivity to carrier Doppler shift.

The acquisition statistic was computed from sums of squares of in-phase and quadrature accumulations and from sums of products of in-phase accumulations with quadrature accumulations. These accumulations were employed in a Neyman-Pearson-type statistic that integrated over chip sign uncertainties by treating each sign as being equally probable. The uncertainty of the BOC phase and the carrier Doppler shift were addressed by performing a brute-force search over predicted ranges for these parameters. The unknown signal amplitude A was removed from the problem by developing a "locally most powerful" hypothesis test statistic. The unknown initial carrier phase ϕ_0 was determined using an analytic optimization that employed products of in-phase accumulations with quadrature accumulations. This optimization is believed to further increase the statistic's sensitivity to carrier Doppler shift.

Search Strategy and Results. We searched for the GIOVE-A signal on a grid in the space of BOC phases and carrier Doppler shifts. The Doppler shift grid was centered on the value predicted by GIOVE-A's NORAD ephemerides, and the grid range was based on estimates of the uncertainties in the ephemerides and in the receiver clock frequency. The grid's BOC phase range covered one full BOC period. The search started with a coarse acquisition on 200 milliseconds of data and finished with a fine acquisition on 1 second of data.

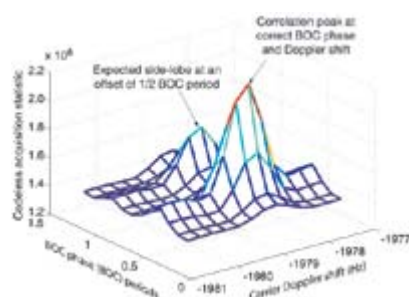


FIGURE 4 presents the results of a fine acquisition based on 1 second of data from March 8. The figure shows a 2-dimensional plot of the acquisition statistic vs. the BOC phase and the carrier Doppler shift. The plot's distinct peak indicates that the GIOVE-A signal was present. The signal's BOC phase and carrier Doppler shift were determined from their values at this peak.

Code Breaking

Figure 4 Fine-scale estimation of BOC phase and Doppler

We realized that removal of the carrier and the BOC modulation would leave us with a signal whose only

shift based on the codeless acquisition statistic

components were the PRN codes and noise. Deriving this signal was our next step.

In-Phase Accumulation. We obtained the signal by computing 1.023 MHz accumulations that were in-phase with the estimated carrier signal. The original 1.023 MHz in-phase and quadrature accumulations that produced the acquisition peak in Figure 4 were rotated by the optimal initial carrier phase φ_{0opt} in order to produce the new in-phase accumulations.

An early indication of the structure of the GIOVE-A signal came from a plot of the circular autocorrelation function of the rotated in-phase accumulations, which is shown in **FIGURE 5** for a 2-second batch of data from March 8. Its high central peak at zero delay is mainly the result of a powerful noise component - the signal-to-noise ratio (SNR) of the accumulations is -5.5 dB. The secondary peaks at multiples of 200 milliseconds are caused by the L1-C pilot signal. Many of the smaller peaks between the 200-millisecond peaks occur at regular intervals of 4 milliseconds—that is, at the period of the L1-B PRN code.

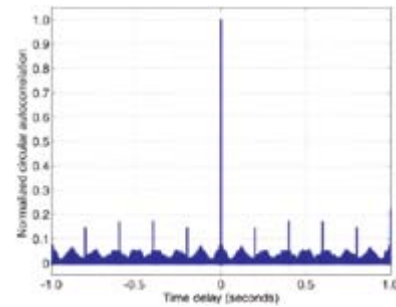


Figure 5 Normalized circular autocorrelation of 1.023 MHz in-phase accumulations of the GIOVE-A signal

The peaks at 200 milliseconds were a surprise. Before seeing this plot, we had learned from Galileo documentation that the L1-C PRN code period was 100 milliseconds, but these peaks clearly indicated a 200-millisecond period. The positive bias of the smaller peaks that were separated by 4 milliseconds was a second surprise. This sign constancy indicated that the L1-B data bits were primarily of a single sign.

Approximate PRN Code Timing. To determine and remove the data symbols and the secondary code chips, we first needed rough estimates of the start/stop times of the L1-B code periods. We estimated them by using a differential analysis to look for times of probable data symbol transitions on the L1-B signal. This analysis computed the following differential time history:

$$\Delta_m = \sum_{j=m}^{m+4091} (I_j - I_{j+4092})^2 \text{ for } m = 1, 2, 3, \dots$$

(3)

where I_j is the j -th 1.023 MHz in-phase accumulation and m is a candidate index of the start of an L1-B PRN code period. Plots of Δ_m vs. m had high values if m was the accumulation index of the first chip of an L1-B PRN code period and if the two successive L1-B data symbols that started at indices m and $m+4092$ had opposite signs. Conversely, these plots took on low values at the start of a pair of PRN code periods that had equal data symbol signs. Noise made it impossible to exactly determine the initial sample time of a code period based on a Δ_m vs. m plot, but the occurrence of several peaks and dips at multiples of 4,092 accumulations yielded an estimate of the L1-B PRN code timing that was accurate to better than 1 percent of a code period.

Blind Alleys. We went down two blind alleys on our way to determining the PRN code chips. Both were the result of wrong assumptions about the structure of the L1-C pilot PRN code. We wrongly conjectured that its primary code maintained a length of 4,092 chips and that its 200-millisecond period was caused by a lengthening of the secondary code from 25 chips to 50 chips.

We made an initial attempt to use the I_j accumulations and the approximate times of the L1-B PRN code periods to determine the +1/-1 L1-B data symbols and the +1/-1 L1-C secondary code chips. Our approach was based on the computation of "soft" linear combinations of these values. They were termed "soft" because they contained noise and because they were multiplied by a scale factor that was a function of the signal amplitude and the number of samples in a code period. Each such "soft" linear combination was the correlation between the accumulations in the 0-th code period, which served as a reference period, and those of another code period. We called the correlation associated with the m -th other code period U_m .

Our analysis indicated that there should be three possible nominal levels of U_m : $-U_{nom}$, 0 , and $+U_{nom}$. The value U_{nom} would occur whenever the L1-B data bit d_m and the L1-C secondary code chip s_m had the same sign as they had for the reference code period, $-U_{nom}$ would occur whenever both signs were reversed from their values during the reference period, and 0 would occur whenever one sign was reversed and one sign was the same.

The actual data looked different. It showed noisy U_m values that could be modeled as taking on five possible nominal levels: U_{nom} , $-0.5U_{nom}$, 0 , $+0.5U_{nom}$, and $+U_{nom}$.

This discrepancy led us to conjecture that the signal contained four 4,092-chip PRN codes that carried one data symbol or one secondary code chip per period. This conjecture explained the five nominal levels of U_m . It was tested by computing an orthogonal set of correlations called V_m . V_m was the correlation of the m -th code period with a second reference code period that had been selected so that its U_m value was nominally 0. The value of V_m constituted a different "soft" linear combination of the data symbols and secondary code chips.

The values of V_m were plotted vs. U_m in hopes of confirming the 4-codes conjecture, but the plot served to refute it. A plot of V_m vs. U_m for the March 2 data set is shown in **FIGURE 6**. Note how the points on the plot are organized into groups at the vertices of a diamond and at the centers of two of its sides. The lengths of the diagonals of this diamond are $2U_{nom} \approx 10^5$. If the four-code hypothesis had been correct, then one would expect to see three additional groups of points, one at the origin and two at the centers of the other two sides of the diamond.

This plot led to a new conjecture that the s_m secondary code chips could take on three values: -1, 0, and +1. The red points in Figure 6 corresponded to the zero values. Armed with this hypothesis, we used the lines shown on Figure 6 to discriminate the d_m data symbol

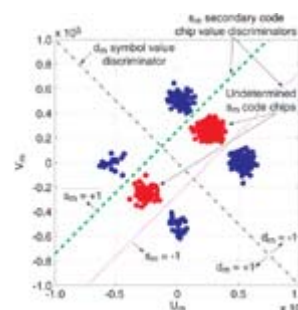
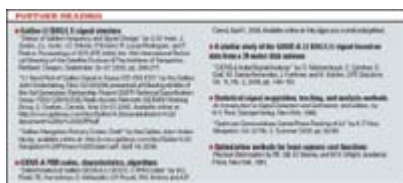


Figure 6 Analysis of data symbols and secondary PRN code chips based on "soft" linear combinations as computed by

values and the s_m secondary code chip values. We found that the s_m correlation analysis chips did have a periodicity of 50, i.e. $s_m = s_{m+50}$. We also found that the zero-valued s_m chips were the odd chips, i.e., $0 = s_1 = s_3 = s_5 = \dots$



Although this hypothesis was wrong, it was completely consistent with the data, and it allowed us to determine the entire L1-B PRN code and half of the L1-C primary PRN code. We did not discover our error until after our initial publication of the PRN codes. In response, a colleague forwarded a paper by *Deutsches Zentrum für Luft- und Raumfahrt's* Oliver Montenbruck et al. (see **FURTHER READING**), which demonstrates that the primary L1-C

Further reading

PRN code is 8,184 chips long rather than 4,092 chips long and that the L1-C secondary code is 25 chips long with no zero-valued chips. In hindsight, we should have realized this fact because the existence of zero-valued chips would have had severe negative ramifications for the ability of the GIOVE-A L1 transmitter to maintain a constant carrier power level.

This new information implied that the red points on Figure 6 corresponded to undetermined values for s_1, s_3, s_5, \dots rather than zero values. We determined these values by choosing new reference PRN code periods for the computation of new U_m and V_m correlations. We chose the new U_m reference period to be the s_i period, and we chose the new V_m reference period to be an odd-numbered period whose new U_m was nominally zero. We generated a new plot like Figure 6 to compute the values for s_1, s_3, s_5, \dots . These new values were identical to s_0, s_2, s_4, \dots or to s_2, s_4, s_6, \dots depending on where the 0-th L1-B code period fell within its corresponding L1-C primary code period.

Determination of Primary PRN Code Chips. We determined the L1-B PRN code, the L1-C primary PRN code, and the PRN code timing simultaneously by solving an optimal estimation problem. The problem amounted to a best fit of the model on the right-hand side of Equation (1) to the measured data on the left-hand side. This problem was reduced to finding the best fit to the following set of measurement model equations for the 1.023 MHz in-phase accumulations:

$$I_j = A_I \left\{ b_{\text{mod}(m+j,4092)} a_{\text{floor}[\{m+j\}/4092]} - c_{\text{mod}(m+j,8184)} s_{\text{mod}(\text{floor}[\{m+j\}/8184],25)} \right\} + v_{Ij} \quad \text{for } j = 0, 1, 2, \dots \quad (4)$$

where m is the true start time of the first L1-B PRN code period, A_I is the unknown accumulation amplitude, and v_{Ij} is accumulation noise.

The unknowns that remained to be estimated were the amplitude A_I , the code timing index m , the L1-B PRN code chips b_0, \dots, b_{4091} , and the L1-C primary PRN code chips c_0, \dots, c_{8183} . The data symbol values d_0, d_1, d_2, \dots and the secondary code chip values s_0, \dots, s_{24} were all assumed to be known exactly from the analysis associated with Figure 6. We estimated the remaining unknowns by minimizing the sums of the squared errors in these equations. The minimization used an optimization scheme that nested a decoupled integer problem for the PRN codes inside a real-valued problem for the accumulation amplitude, which itself was nested inside a brute-force integer optimization for the code timing index.

We solved this optimal estimation problem twice using independent 2-second data sets, one from March 2 and one from March 8. The optimal PRN codes were identical for the two data sets. Next, we evaluated the probability of a chip error in the determined PRN codes using a conservative method. This probability was less than 8.5×10^{-11} .

On April 3, receiver manufacturer NovAtel used the L1-B PRN code that we had determined in their new EuroPak-L1L5E5a receiver to successfully track the GIOVE-A signal, thus confirming our result. Tests on subsequent days also proved successful, but tests on April 13 and April 18 failed to find the signal. These latest results indicate that GIOVE-A does not always broadcast its L1 signal or that its PRN codes have been changed from their March 2 and March 8 values.

Near press time for this article, a new Galileo draft document was published that purported to contain, among other things, the system's 50 L1-B and L1-C primary PRN codes. None of the published codes correlated well with the codes that we determined for GIOVE-A, and the published L1-C codes were only 4,092 chips long, which disagrees with our results.

Conclusions

A method was developed for determining the PRN codes of a Galileo satellite's L1 BOC (1,1) signal. This method involves codeless acquisition, computation of 1.023 MHz baseband in-phase accumulations, and analysis of these accumulations to determine PRN code start times and chip values. These techniques were applied to GIOVE-A data collected using a patch antenna and a digital storage receiver. The PRN codes were determined independently from two sets of 2-second data batches that were recorded on March 2 and March 8. The resulting PRN codes were identical, and the error probability of each chip was less than 8.5×10^{-11} . The data channel's PRN code chips were found to be 1,1,-1,1,1,1,-1,-1,-1,-1, ..., and the pilot channel's chips were 1,1,-1,-1,1,1,-1,-1,-1,-1, ... for the two days in question. Subsequent analysis of the GIOVE-A signal showed that it had a power level only 3.3 dB lower than the strongest GPS L1 C/A signals when viewed at a 45-degree elevation angle, that its structure had the expected properties of a BOC(1,1) signal, and that its Doppler shift was within 10 Hz of the expected value based on NORAD ephemerides.



Richard Langley

AT 05:19 UTC ON DECEMBER 28, 2005, the first Galileo test satellite blasted off from the Baikonur Cosmodrome atop a Soyuz-FG rocket. The rocket's Fregat upper stage placed the 649 kilogram satellite known as GIOVE-A (Galileo In-Orbit Validation Element-A) into a 29,635 kilometer circular orbit with an inclination of about 56 degrees. Built by Surrey Satellite Technology Ltd. of Guildford, England, GIOVE-A's role is to secure the Galileo system's frequencies allocated by the International

Telecommunication Union, validate key technologies, and characterize the radiation environment of the orbits planned for the full constellation which is scheduled to be deployed by 2010.

GIOVE-A carries a pair of redundant rubidium atomic clocks, a navigation signal generation unit, and a laser reflector. (Data from satellite laser ranging stations will help with analyses of satellite orbit and clock variations.) GIOVE-A can transmit two signals at a time from its L-band phased array antenna: either E2-L1-E1 (commonly called L1) and E5, or L1 and E6, using special pseudorandom noise (PRN) codes that are different from the planned Galileo codes. Furthermore, the navigation message broadcast by GIOVE-A is not representative of the structure or content ultimately to be used by Galileo.

The GIOVE-A payload was activated on January 10, 2006, with the first signals broadcast on January 12. Official monitor sites of the transmissions included the Rutherford Appleton Laboratory's Chilbolton Observatory in Hampshire, England, and the European Space Agency's Redu Station in the Ardennes region of Belgium. However, a number of researchers across the globe were interested in acquiring and studying the first Galileo signals. But because the PRN codes to be used by GIOVE-A had not been published, detection and tracking of the signals would not be easy. One could either use a very high gain dish antenna to lift the weak satellite signals out of the background noise or use clever signal manipulation techniques with stored signal samples acquired with a simple low gain antenna. In this month's column, Mark Psiaki and his colleagues at Cornell University describe how they used this latter approach to acquire and analyze the L1 signals transmitted by GIOVE-A.

"Innovation" is a regular column featuring discussions about recent advances in GPS technology and its applications as well as the fundamentals of GPS positioning. The column is coordinated by Richard Langley of the Department of Geodesy and Geomatics Engineering at the University of New Brunswick, who appreciates receiving your comments and topic suggestions. To contact him, see the "Columnist" section in this issue.

MARK L. PSIAKI received a B.A. degree in physics and M.A. and Ph.D. degrees in mechanical and aerospace engineering from Princeton University in 1979, 1984, and 1987, respectively. He joined Cornell University's Sibley School of Mechanical and Aerospace Engineering in 1986. His primary research activities lie in applications of estimation theory to GNSS and other aerospace systems.

TODD E. HUMPHREYS is a graduate student in the Sibley School of Mechanical and Aerospace Engineering at Cornell University. He received his B.S. and M.S. degrees in electrical and computer engineering from Utah State University in 2000 and 2003, respectively. His research interests are in estimation and filtering, spacecraft attitude determination, GPS technology, and GPS-based study of the ionosphere and neutral atmosphere.

SHAN MOHIUDDIN received a B.S. degree in aerospace engineering from Virginia Tech in 2003. He interned at NASA Goddard Space Flight Center in Greenbelt, Maryland, before entering the Ph.D. program in Cornell University's Sibley School of Mechanical and Aerospace Engineering. He has been a NASA Graduate Student Researchers Program Fellow since 2004. His research focuses on satellite navigation algorithms and GNSS receiver technology.

STEVEN P. POWELL is a senior engineer with the Space Plasma Physics Group in the Department of Electrical and Computer Engineering at Cornell University. He has been

involved with the design, fabrication, testing, and launch activities of many scientific experiments flown on high-altitude balloons, sounding rockets, and satellites. He has designed ground-based and space-based GPS receiving systems primarily for scientific applications. He earned B.S. and M.S. degrees in electrical engineering from Cornell University in 1982 and 1983, respectively.

ALESSANDRO P. CERRUTI is a graduate student in the Space Physics and Engineering Group in the School of Electrical and Computer Engineering at Cornell University. He received both B.S. and M.Eng. degrees in electrical and computer engineering at Cornell University in 2002 and 2003, respectively. His primary research is in space weather and its effects on GNSS receiver operation.

PAUL M. KINTNER, JR. received a B.S. degree in physics from the University of Rochester and a Ph.D. in physics from the University of Minnesota in 1968 and 1974, respectively. He joined the faculty of Cornell University's School of Electrical and Computer Engineering in 1981. He has been the principal investigator for numerous NASA ionospheric sounding rockets and led the Living With a Star: Geospace Mission Definition Team. His primary research activities concern space weather and its effects on GNSS and other systems.